25th International Congress on Sound and Vibration
8-12 July 2018 HIROSHIMA CALLING
ICSV25

# ERROR MICROPHONE LOCATION STUDY FOR AN EIGHT-CHANNEL ANC SYSTEM IN FREE SPACE

Jiancheng Tao, Qin Guo

*Key Laboratory of Modern Acoustics and Institute of Acoustics, Nanjing University, Nanjing 210093, China*

*email: jctao@nju.edu.cn*

Guoyong Jin

*College of Power and Energy Engineering, Harbin Engineering University, Harbin 150001, China*

Xiaojun Qiu

*Centre for Audio, Acoustics and Vibration, Faculty of Engineering and IT, University of Technology Sydney, NSW 2007, Australia*

The location of error microphones is one key factor that determines the performance of a multichannel active noise control (ANC) system in terms of global sound power reduction when the number and the location of secondary sources are fixed. In a single channel ANC system, the optimal error microphone location is on a line that is nearly perpendicular to the secondary and primary source axis and closer to the secondary source. This paper investigates the optimal location of the error microphones in an 8-channel ANC system in free space. It is demonstrated that good noise reduction performance can be achieved by placing the error microphones between the primary source and secondary sources and closer to the secondary sources in the low frequency range. Experiments conducted on a gearbox for low frequency noise control show that the averaged sound level reduction at the observation locations 2 meters away is 5.2 dB when the error microphones are placed at 0.2 m inside the secondary source surface.

Keywords: multichannel ANC systems, error microphone location

## 1. Introduction

Error sensing strategy is an important issue in active noise control (ANC) systems, which determines the noise reduction performance and physical compactness, especially after the secondary sources are installed [1]. For a monopole primary source and a dipole like pair of primary sources in free space, different error sensing strategies have been compared and it is found that minimising the sum of the mean active sound intensity in the radial direction is the best strategy when the error

sensors are quite close to the control sources [2]. For the structural noise sources, the vibration information on the structural surface, such as the amplitude of vibration modes or radiation modes has been proposed to estimate the sound power to be depressed [3, 4].

The sound pressure sensing strategy, which employs the sound pressure or the sum of squared sound pressure at error microphones as the cost function, has been widely used in practical multichannel ANC systems for sound radiation control due to the implementation convenience [5, 6]. The acoustic power attenuation resulting from minimizing the acoustic pressure amplitude at a single error microphone has already been presented in the textbook [7]. It is proposed that the acoustic power attenuation achieved when minimizing the acoustic pressure at the sensor(s) varies rapidly with location when placing the error sensor(s) in the near field of the sources, especially the primary source. The sound power control for a single primary source with two secondary sources has also been investigated, and the optimal distance between the primary source and the error microphone is 0.618 times the distance between the primary source and secondary sources when sound sources are in straight-line arrangement [8].

This paper is a following work based on reference [9], and the effect of error microphone locations is investigated when 8 secondary sources are placed at the vertexes of a cuboid centred at the primary source. First, the theoretical model of the 8-channel ANC system in the cube vertex configuration is discussed. Then simulations for both the cube and cuboid vertex configurations are performed. Finally, experiments in cuboid vertex configuration are presented to verify the noise reduction performance with different error microphone locations.

## 2. Theoretical model

The 8-channel ANC system in free space investigated in this paper is shown in Fig. 1, where 8 secondary sources and 8 error microphones are distributed on the vertexes of two cubes centred at the primary monopole source. Each error microphone is on the line crossing its neighbouring secondary source and the primary source. The distance between each error microphone and the primary source is $d_{\mathrm{pe}}$, and the distance between each secondary source and the primary source is $d_{\mathrm{ps}}$. If $d_{\mathrm{pe}} < d_{\mathrm{ps}}$, the error microphones are placed between the primary source and the secondary sources.

Assuming all the sound sources in Fig. 1 are monopoles, the sound power with active control can be formulated as [1]

$$W = \mathbf{Q}_{\mathrm{s}}^{\mathrm{H}}\mathbf{A}\mathbf{Q} + \mathbf{Q}_{\mathrm{s}}^{\mathrm{H}}\mathbf{b} + \mathbf{b}^{\mathrm{H}}\mathbf{Q}_{\mathrm{s}} + c\,, \tag{1}$$

where $\mathbf{Q}_{\mathrm{s}}$ is the strength vector of the secondary sources, $\mathbf{A}$ is an 8 × 8 matrix composed by the radiation resistances between two corresponding secondary sources, $\mathbf{b}$ is an 8 × 1 vector consisting of the mutual radiation resistances from the primary source to secondary sources, and $c$ is the sound radiation power of the primary source without control. The elements of the matrixes in Eq. (1) are $A_{ij} = 0.5Z_0\mathrm{sinc}(kd_{\mathrm{ss},ij})$, $b_i = 0.5Z_0Q_{\mathrm{p}}\mathrm{sinc}(kd_{\mathrm{ps}})$, and $c = 0.5Z_0Q_{\mathrm{p}}^2$, where $Z_0 = \omega^2\rho_0/4\pi c_0$ is the self-radiation resistance of a monopole in free space, $\omega$ is the angular frequency, $\rho_0$ is the air density, $c_0$

is the sound speed, $k = \omega/c_0$ is the wave number, $d_{ss,ij}$ is the distance between the $i$th and $j$th secondary sources, $Q_p$ is the strength of the primary source, and the function $\mathrm{sinc}(x) = \sin(x)/x$.

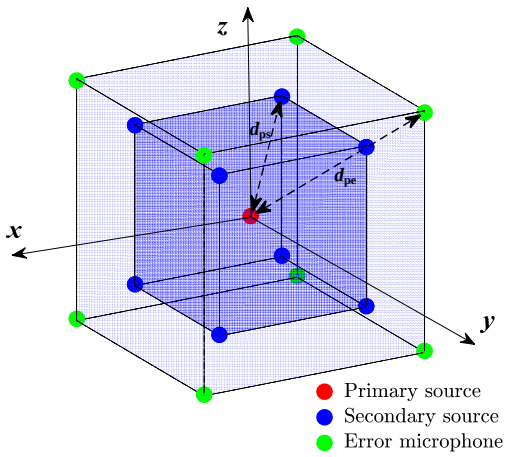


Figure 1: Sketch map of the 8-channel ANC system in free space.

The noise reduction with active noise control is

$$NR = -10\log_{10}\left[\frac{W}{W_0}\right], \tag{2}$$

where $W_0$ is sound power without control and $W_0 = c = 0.5Z_0Q_p^2$. If the total sound power of both primary and secondary sources is adopted as the cost function, the optimal noise reduction is

$$NR_{\mathrm{opt}} = -10\log_{10}\left[1-\frac{\mathbf{b}^{\mathrm{H}}\mathbf{A}^{-1}\mathbf{b}}{c}\right]. \tag{3}$$

Instead of the total sound power, the sum of squared sound pressure level at error microphones is always employed as the cost function in applications due to the implementation convenience. Considering the symmetry of the system in Fig. 1, the strengths of all secondary sources are assumed to be $Q_s$, and the sound pressure at any error microphones can be formulated as

$$p = \frac{\mathrm{j}\omega\rho_0 Q_p e^{-\mathrm{j}kd_{pe}}}{4\pi d_{pe}} + \sum_{i=1}^{8}\frac{\mathrm{j}\omega\rho_0 Q_s e^{-\mathrm{j}kd_{se,i}}}{4\pi d_{se,i}}, \tag{4}$$

where $d_{se,i}$ is the distance between one error microphone and the $i$th secondary source. In the minimization of the sum of squared sound pressure at error microphones, the optimal secondary source strength can be solved by assuming Eq. (4) being zero and the result is

$$Q_s = -Q_p\frac{e^{-\mathrm{j}kd_{pe}}}{d_{pe}}\left[\sum_{i=1}^{8}\frac{e^{-\mathrm{j}kd_{se,i}}}{d_{se,i}}\right]^{-1}. \tag{5}$$

Substituting Eq. (5) into Eq. (1), the total sound power with control is

$$W = c\left\{1 + 16\,\mathrm{Re}\left[\frac{Q_\mathrm{s}}{Q_\mathrm{p}}\right]\mathrm{sinc}\left(kd_\mathrm{ps}\right) + 8\left|\frac{Q_\mathrm{s}}{Q_\mathrm{p}}\right|^2 \sum_{i=1}^{8}\mathrm{sinc}\left(kd_{\mathrm{ss},i}\right)\right\}, \tag{6}$$

where Re[] denotes the real part in the square brackets, | | is the modulo operator, $d_{\mathrm{ss},i}$ is the distance between one secondary source and the $i$th secondary source.

If the frequency is sufficiently low, the wavelength $k$ decreases to zero and all the sinc($x$) function terms approach 1. Therefore, Eq. (5) can be simplified as

$$Q_\mathrm{s} = -Q_\mathrm{p}\frac{1}{d_\mathrm{pe}}\left[\sum_{i=1}^{8}\frac{1}{d_{\mathrm{se},i}}\right]^{-1}. \tag{7}$$

Substituting Eq. (7) into Eqs. (1) and (2), the noise reduction is

$$NR = -10\log_{10}\left[\frac{W}{W_0}\right] = -20\log_{10}\left[1 - \frac{8}{d_\mathrm{pe}}\left(\sum_{i=1}^{8}\frac{1}{d_{\mathrm{se},i}}\right)^{-1}\right]. \tag{8}$$

To maximize the noise reduction in Eq. (8), the distance $d_{\mathrm{se},i}$ should be chosen as large as possible, or the distance $d_\mathrm{pe}$ should be chosen to satisfy

$$d_\mathrm{pe} = 8\left(\sum_{i=1}^{8}\frac{1}{d_{\mathrm{se},i}}\right)^{-1}. \tag{9}$$

Consider the symmetrical cube vertex configuration of the secondary sources and error microphones in Fig. 1, it can be obtained that the optimal distance $d_\mathrm{pe} = 0.787 d_\mathrm{ps}$ from Eq. (9) and the corresponding secondary source strength in Eq. (7) equals $-Q_\mathrm{p}/8$. The upper limit of the noise reduction with the sound pressure sensing strategy is the noise reduction with the sound power control.

## 3. Numerical Simulations

Consider the 8-channel ANC system shown in Fig. 1, the distance between the primary source and each secondary source is fixed as 1 m. The noise reduction with different error microphone locations when the sum of the squared sound pressure is adopted as the cost function calculated is shown in Fig. 2. Three different frequencies, 57 Hz, 99 Hz and 142 Hz were chosen in the simulations according to the experiment setup in section 4 and the global control requirement that distance $d_\mathrm{ps}$ should be less than half wavelength is meet at these frequencies [7]. Fig. 2 shows that the noise reduction has an obvious peak within the range $r_\mathrm{pe} < 1$ m, where the error microphones are placed between the primary source and the secondary sources. When the distance $r_\mathrm{pe}$ is sufficiently large (beyond 1.5 m), the noise reduction increases and converges with $r_\mathrm{pe}$. As discussed on Eq. (8), the maximal noise reduction occurs when the error microphones are placed infinitely far or at a specific location satisfying Eq. (9).

The maximal noise reduction with sound pressure sensing strategy and the corresponding optimal $r_\mathrm{pe}$ at different frequencies are shown in Fig. 3. The optimal $d_\mathrm{pe}$ is in the range between 0.7 m and 0.9 m at most frequencies, and converges to 0.787 m when the frequency decreases to zero. The

noise reduction with optimally placed error microphones is very close to the noise reduction with sound power control in the investigated frequency band.

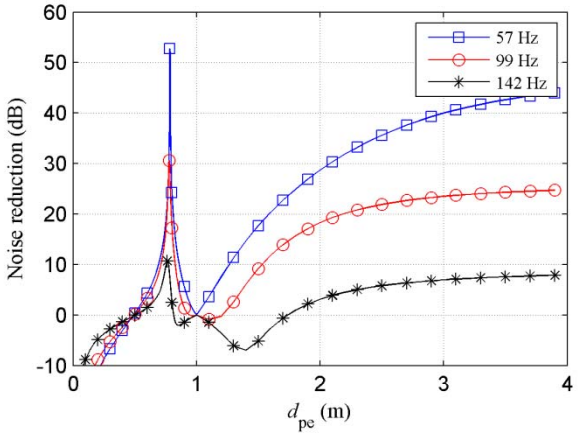


Figure 2: Noise reduction with different error microphone locations at 57 Hz, 99 Hz and 142 Hz.

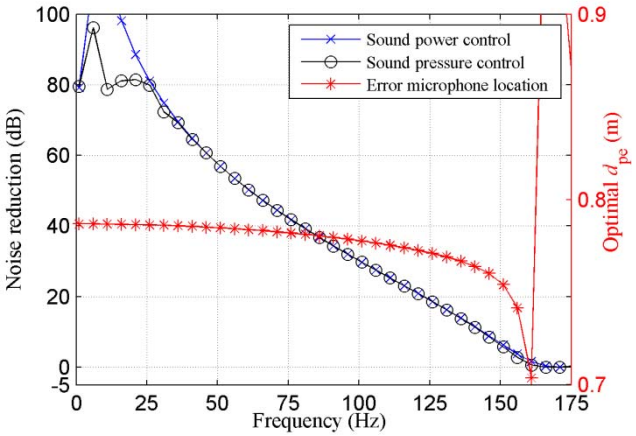


Figure 3: Maximal noise reduction and the corresponding optimal $d_{pe}$ with sound pressure sensing strategy.

In some applications, the secondary sources and error microphones cannot be placed at cube vertexes due to the space constraint and the cuboid vertex configuration needs to be further considered. Assume that 8 secondary sources are placed at the vertexes of a cuboid, which centred at the primary source with the dimensions of 1.00 m × 0.72 m × 0.72 m. The distance between each secondary source and the primary source is about 0.71 m. The error microphones are also located on the lines determined by the secondary sources and the primary source with an equal distance to the primary source.

The estimated noise reduction with different error microphone locations is shown in Fig. 4, where the noise reduction decreases with the frequency. The maximal noise reduction is achieved when the error microphones are placed 0.4 m outside the secondary source surface ($d_{pe}$ = 1.11 m). If the error microphones need to be placed between the primary source and the secondary sources to

make the system compact, the error microphones are suggested to be placed 0.2 m inside the secondary source surface ($d_{pe}$ = 0.51 m) to achieve better noise reduction performance.

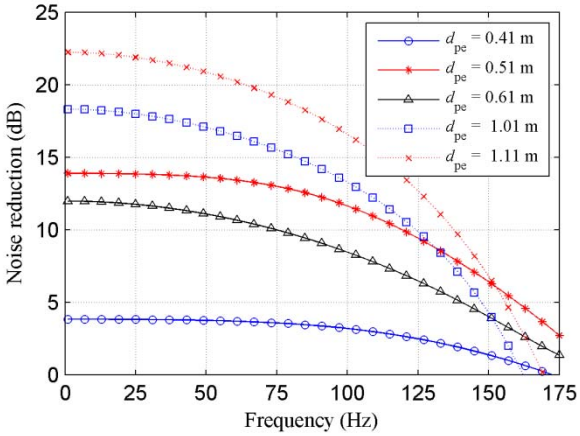


Figure 4: Noise reduction with different error microphone locations in cuboid vertex configuration.

## 4. Experiments

Experiments were conducted in an anechoic chamber in Harbin Engineering University. The recorded noise from a gearbox with the fundamental frequency of 14.2 Hz was used to drive a loudspeaker as the primary source. Considering that mufflers exist at two sides of the primary source, 8 secondary sources were placed at the vertexes of a cuboid cantered at the primary source as shown in Fig. 5, and the cuboid dimension was same as that used in the simulation (1.00 m × 0.72 m × 0.72 m). All the loudspeakers were self-made and their volume was 20.0 cm × 20.0 cm × 22.0 cm. In the experiments, a multichannel ANC controller with the embedded waveform synthesis algorithm [10] was employed and 9 harmonic components around 57 Hz, 71 Hz, 85 Hz, 100 Hz, 114 Hz, 128 Hz, 142 Hz, 156 Hz and 170 Hz were chosen as the control targets.

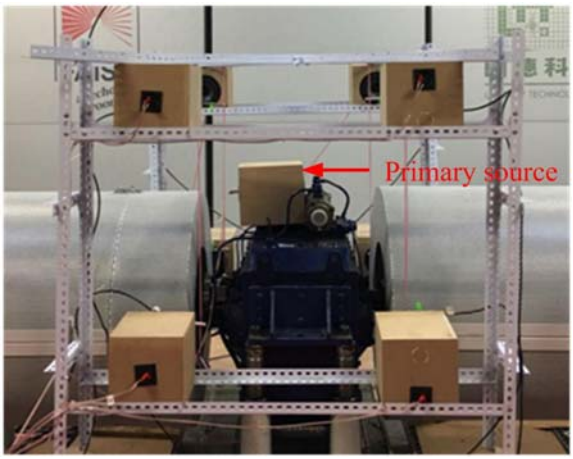


Figure 5: Experimental setup.

When 8 error microphones were placed 20 cm inside the secondary source surface, the averaged sound pressure without and with control is shown in Fig. 6(a), where the sound pressure at the target frequencies are depressed almost to the background level. Fig. 6(b) shows the averaged sound pressure at 7 observation locations 2 meters away around the primary source. The measured sound reduction is over 4.3 dB (the averaged value is 5.2 dB) at the target frequencies except 114 Hz and 142 Hz, where the primary sound pressure level is at least 20 dB lower than the highest peak value.

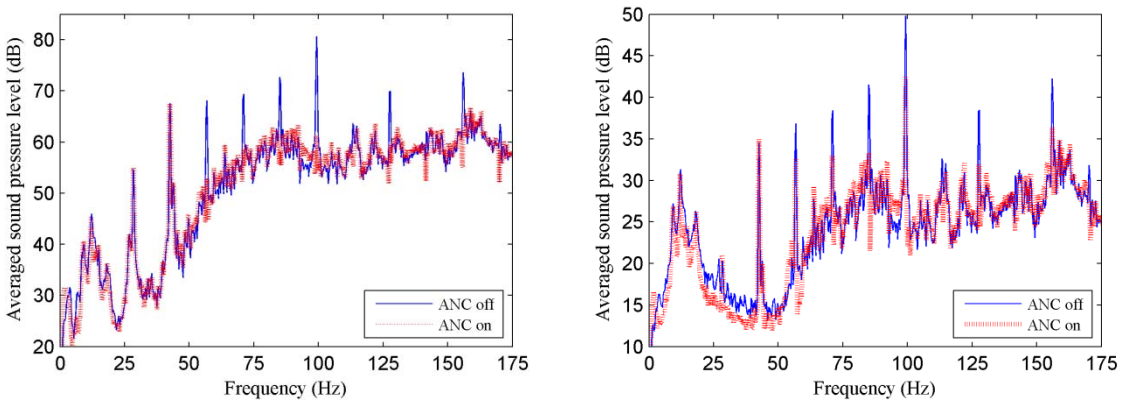


Figure 6: Averaged sound pressure level with and without control when the error sensors are 20 cm inside the secondary source surface (a) at error microphones (b) at observation locations

The reduction of the averaged sound pressure level at observation locations is listed in Table 1. It is clear that the best reduction performance is achieved when the distance $d_{pe}$ = 0.51 m, which means that the optimal location of the error microphones is between the primary source and secondary sources in the experiments. This is different from the simulation results shown in Fig. 4 where the optimal distance is $d_{pe}$ = 1.11 m. The reason for this deviation maybe that the scattering of the gearbox and mufflers are not considered in the simulations. However, it is validated that good noise control performance can be achieved by placing the error microphones between the primary source and secondary sources and closer to the secondary sources.

Table 1: Measured reduction of the averaged sound pressure level at observation locations

| $f$ (Hz) / $NR$ (dB) / $d_{pe}$ (m) | 56.8 | 71 | 85 | 99 | 114 | 128 | 142 | 156 | 170 |
|---|---|---|---|---|---|---|---|---|---|
| 0.41 | −1.4 | −1.3 | 3.2 | 2.2 | 0.0 | 1.0 | −1.0 | 0.8 | 1.9 |
| 0.51 | 4.3 | 5.8 | 8.2 | 7.4 | 2.7 | 6.9 | 0.3 | 5.8 | 5.5 |
| 0.61 | 4.6 | 8.2 | 9.8 | 8.7 | 4.7 | 2.5 | −0.5 | 1.2 | −0.6 |
| 1.01 | 6.7 | 3.8 | 4.8 | 4.9 | 2.0 | 0.8 | −1.7 | −2.9 | −3.5 |
| 1.11 | 7.8 | 4.2 | 6.7 | 6.9 | 3.5 | 2.0 | 0.0 | −2.2 | −4.1 |

## 5. Conclusions

The location of error microphones in an 8-channel active noise control system is investigated in terms of global sound power reduction. It is demonstrated that good noise reduction performance can be achieved by placing the error microphones between the primary source and secondary sources and closer to the secondary sources. If the system is symmetrical about the primary source and in the cube vertex configuration, the optimal distance between the primary source and the error microphones is about 0.787 times of the distance between the primary source and the secondary sources when the frequency is sufficiently low. Experiment results show that a sound level reduction of 5.2 dB is obtained at the observation locations when the error microphones are placed 0.2 m inside the secondary source surface.

## REFERENCES


1 Nelson, P. A. and Elliott, S. J., *Active Control of Sound*, Academic Press, (1992).

2 Qiu, X., Hansen, C. H. and Li, X., A Comparison of Near Field Acoustic Error Sensing Strategies for the Active Control of Harmonic Free Field Sound Radiation, *Journal of Sound and Vibration*, **215**, 81–103, (1998).

3 Snyder, S. D. and Tanaka, N, On Feedforward Active Control of Sound and Vibration Using Vibration Error Signals. *Journal of the Acoustical Society of America*, **94**(4), 2181–93, (1993).

4 Elliott, S. J. and Johnson, M. E. Radiation Modes and the Active Control of Sound Power, *Journal of the Acoustical Society of America*, **94**(4), 2194–204, (1993).

5 Tao, J., Wang, S., Qiu, X. and Pan, J., Performance of a multichannel active sound radiation control system near a reflecting surface, *Applied Acoustics*, **123**, 1–8, (2017).

6 Tao, J., Qiu, X. and Pan, J., Control of Transformer Noise Using an Independent Planar Virtual Sound Barrier, *Proceedings of Acoustics 2015*, Hunter Valley, Australia, 15–18 Nov, (2015).

7 Hansen, C. H., Snyder, S. D., Qiu, X., et al., *Active Control of Noise and Vibration* (2nd edition), E&FN SPON, (2013).

8 Hayashi, T., Enamito, A. and Suzuki, S., Active Acoustic Power Control of a Single Primary and Two Secondary Sources by the Acoustic Nodal Point Method. *Journal of the Acoustical Society of Japan*, **16**(4), 213–221, (1995).

9 Guo, Q., Tao, J., Jin, G. and Qiu, X., Physical System Optimization in Global Active Radiation Control with Space Constraint, *Proceedings of the 46th international congress and exposition on noise control engineering*, Hong Kong, 27–30 Aug, (2017).

10 Qiu, X., Li, X., Ai, Y. and Hansen, C., A Waveform Synthesis Algorithm for Active Control of Transformer Noise: Implementation, *Applied Acoustics*. **63**, 467–479, (2002).